Selecting an optimum electrolyte for zinc chloride electrolysis

P. M. COPHAM, D. J. FRAY

Department of Materials Science and Metallurgy, University of Cambridge, Pembroke Street, Cambridge CB2 3QZ, UK

In order to be able to select the optimum composition of an electrolyte in the $ZnCl_2$-$NaCl$-KCl system, the conductivity, surface tension and density were measured for a series of melts in the composition range 28–50 mol % $ZnCl_2$, 0–62 mol % KCl and 0–62 mol % $NaCl$. It was found that the results could be correlated with the phase diagram and that the difference between the temperature of measurement and the liquidus or glass transition point was an important parameter in defining the properties. The optimum composition was found to be 40 mol % $ZnCl_2$, 30 mol % KCl and 30 mol % $NaCl$.

1. Introduction

A knowledge of the electrochemical and physical properties (such as electrical conductivity, surface tension and density) is necessary when considering the optimum composition of a melt for an electrolysis cell. Conductivity is generally considered the most important property because of its effect on ohmic losses in the melt; it should therefore be kept as high as possible [1, 2]. The conductivity of pure molten salts depends on the size of the cations, the degree of ionic character of the bonds and hence the interaction of the ions and their nearest neighbours [1, 2]. The alkali halides show a steady decrease in conductivity from the lithium halide to the caesium halide due to the increasing size of the cation. They are relatively good conductors due to the high degree of ionic character in the bonding, whereas salts with predominantly covalent bonding, for example mercury halides, are poor conductors. Zinc chloride is another poor conductor, particularly close to its melting point where the conducting entities are in equilibrium with a mainly molecular structure. As the temperature increases, however, this structure rapidly breaks down and the proportion of ions, including Zn^{2+}, $ZnCl^+$, $ZnCl_3^-$ and $ZnCl_4^{2-}$, becomes larger, rapidly increasing the conductivity [2]. The addition of alkali halides to zinc chloride also greatly increases the conductivity. This again results from the breakdown of the zinc chloride network structure to give a combination of zinc chloride polymer fragments, alkali metal cations and complex zinc anions [3].

When mixing salts, conductivities are not generally additive, the deviations from ideal conductivity isotherms, being explained in terms of ionic interactions, sometimes with the formation of complex species [4]. The ideal equivalent conductivity isotherm for a binary mixture is taken to be linear with respect to molar composition. The majority, however, deviate negatively from this, although a few systems have positive deviations [2, 5]. Mixtures of potassium chloride and zinc chloride demonstrate the effect of complexing [6]. The isotherms of equivalent conductivity show maximum negative deviations at approximately 0.71 mol fraction of potassium chloride, corresponding closely to the composition $2KCl . ZnCl_2$.

The interfacial tensions between the liquid metal, the gas and the melt influence the ease with which one phase is dispersed within the other [7] and is, therefore, an important factor affecting the stability of the metal-electrolyte interface and the ease of mixing of the products. An increase in surface tension will tend to reduce globule formation and therefore have a beneficial effect on cell operation [7]. Generally, surface tension, σ, decreases with temperature [2, 8, 9, 10–14] for most molten salts.

The separation of the products in most electrolysis cells depends on the density between the salt and the products [15]. A knowledge of the density is therefore important in order to ensure that an adequate density difference is maintained in the melt.

The density, ρ, of molten salt generally [2, 3, 6–9] decreases linearly with increasing temperature. In the case of zinc chloride a change in the slope of the plot of density versus temperature occurs at 643 K [12]. This is thought to be due to fragments of the network structure linking up on cooling to produce quasi-crystalline clusters. The addition of a few mol % of alkali metal chlorides is sufficient to break up the network structure to form complex ions, resulting in a linear plot. The complex ions result in an increasingly reduced partial molar volume of zinc chloride on going from lithium to caesium chloride. With increasing temperature, however, these ions become less stable and the partial molar volumes will tend to approach a value independent of the added alkali chloride.

Recently, the United States Bureau of Mines [16–18] examined the various factors affecting the production

of zinc from a mixture of $ZnCl_2$–KCl–NaCl. Results, from an electrowinning cell, showed that current efficiencies decreased with an increase in either the temperature or zinc chloride content, fuming increased with temperature in the order KCl–$ZnCl_2$, $LiCl$–$ZnCl_2$, $ZnCl_2$, and whilst the KCl–$ZnCl_2$ melt was also the least hygroscopic, it did not have a particularly high conductivity. On the basis of these results a melt of composition 29.9 mol % $ZnCl_2$, 54.6 mol % KCl and 15.5 mol % NaCl was chosen for electrolysis in a 500 A cell, this melt having the best balance with regard to fuming, moisture absorption, dissolution of metal, conductivity and energy efficiency at 773 K.

As can be judged from this brief introduction, it is not possible to predict the conductivity, density or surface tension for a given composition and, therefore, measurements are needed on the $NaCl$: KCl : $ZnCl_2$ system to optimize the electrolyte for the electrolysis of zinc chloride.

2. Experimental procedure and details

2.1. Measurements of conductivity

The measurements were carried out using a capillary cell, with a relatively high cell constant, K, connected to a Wayne Kerr Universal Bridge [2, 19]. The cell was first calibrated using a standard solution of known conductivity, κ, from which the cell constant was calculated.

$$K = \kappa/c \qquad (1)$$

where c = conductance measured by the bridge in Ω^{-1}.

The conductivity cell consisted of a U-shaped silica capillary tube, 140 mm long and 2 mm in internal diameter, with a reservoir at each end to contain the melt (Fig. 1). A cylindrical platinized platimun electrode was held in place at each end of the capillary by a platinum wire contact which was cemented to the wall of the reservoir with Autostic.

The cell was partially immersed in a molten salt bath to produce an even temperature distribution. The
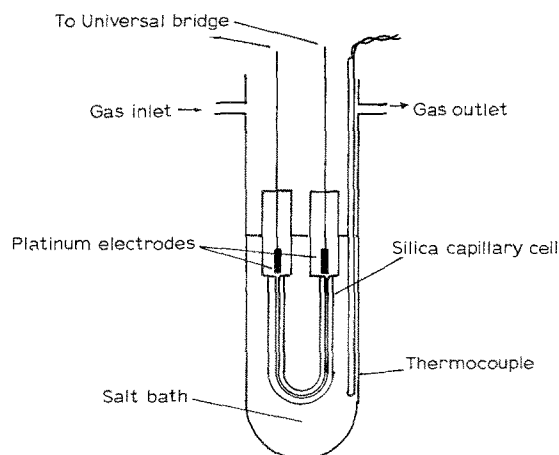

Fig. 1. Schematic diagram of the electrical conductivity cell.

bath was contained in a silica tube which had a gas inlet and outlet to provide a dry nitrogen atmosphere.

The salt mixtures were weighed out according to the nominal composition required, loaded into the cell, together with 1 wt % NH_4Cl to react with any zinc oxide and to dry the salt. After holding at 433 K overnight, the cell was then placed in the molten salt bath, at the maximum temperature in the range to be studied to ensure that all the NH_4Cl sublimed. The system was kept under a nitrogen atmosphere in a dry box [20] and the melt was left to stand for approximately one hour to allow the temperature to stabilize and the NH_4Cl to react. Measurement of the conductance and capacitance of the system was then carried out using the Universal bridge.

At the end of each experiment the melt was recovered and sent for analysis to determine the true composition and ensure that no NH_4Cl remained.

2.2. Measurement of surface tension and density

The surface tension and density were both measured using the maximum bubble pressure method where the maximum excess for pressure, p, required to produce a bubble of radius r, at a depth in beneath the liquid surface is measured. The pressure can be expressed as

$$p = \rho g h + 2\sigma/r \qquad (2)$$

where ρ = density of the liquid, g = acceleration due to gravity, and σ = surface tension

The pressure is at a maximum when r is at a minimum, that is, when the radius of the bubble is equal to the tube radius. The surface tension can therefore be obtained by measuring the difference in the maximum excess pressure, Δp, required to produce a bubble in two tubes of different radii at the same depth beneath the liquid surface. Hence equation 2 becomes

$$\Delta p = 2\sigma \left(\frac{1}{r_1} - \frac{1}{r_2} \right) \qquad (3)$$

where r_1 and ρ_2 are the tube radii. Rearranged, the surface tension is given by

$$\sigma = \frac{\Delta p}{2\left(\dfrac{1}{r_1} - \dfrac{1}{r_2} \right)} \qquad (4)$$

Similarly, the density can be obtained by measuring the difference in the maximum pressure required to produce a bubble in the same tube at two different depths. Equation 2 now becomes:

$$\Delta p = \rho g (h_1 - h_2) \qquad (5)$$

where h_1 and h_2 are the depths. Rearranged, the density is given by

$$\rho = \frac{\Delta p}{g(h_1 - h_2)} \qquad (6)$$

When calculating the difference in pressure to obtain the density, a correction must be included to take

account of the increased displacement of liquid at the greater immersion depth.

The apparatus employed consisted of two silica capillary tubes, with different diameters, immersed in the melt which was contained in a recrystallized alumina crucible, 50 mm high and 35 mm internal diameter. The crucible was mounted on a pyrophillite platform in a vertical furnace with a long, stable hot zone. The two silica tubes (1.1 mm and 2.2 mm internal diameter) and a chromel/alumel thermocouple protected by a silica sheath were supported in a frame which rested on top of the furnace. This allowed the tubes and the thermocouple to be lowered into the melt by means of an adjusting screw, one turn resulting in a height change of 2.0 mm. The ends of the silica capillary tubes were polished flat to ensure a sharp edge to enable the bubble to detach itself.

The gas used in the experiments was high purity argon which was first dried by passing it through concentrated sulphuric acid and then a type 4A molecular sieve. The gas entered the distribution manifold through an Edwards high vacuum needle valve to give the required control at low gas flow rates. A two-way tap on the manifold enabled the gas to be directed through either of the two capillary tubes. An outlet tap on the manifold was connected to a Furness Controls PPFA-FCO 60 microanometer which was capable of measuring pressures of up to 100 mm H_2O with a resolution of better than 0.5 mm H_2O. The manometer was then connected to the 'X' input of an X-T chart recorder to enable greater accuracy in the readings which were, of necessity, dynamic in nature. The output from the manometer was 1 mV d.c. per mm H_2O.

The correction to take into account the displacement of the molten salt by the capillary tubes when measuring the true depth of immersion was calculated. This had been checked previously by low temperature experiments using the methanol/water system [21, 22].

The crucible was filled with 100 g of the salt mixture with the nominal composition required, together with 1 g of NH_4Cl reducing/drying agent. This was heated up to the highest temeprature required for the experiment, in a pre-heated furnace and under an argon atmosphere. The experiments were carried out at the higher temperatures first to ensure that all the NH_4Cl sublimed. The melt was allowed to stabilize for 30 minutes before beginning the experiment, to ensure that the NH_4Cl reaction was complete.

The tubes were then lowered into the melt and the flow rate adjusted to give a constant value of maximum pressure at a bubble rate of approximately 5 min^{-1}. Bubbles were blown from one tube then the other every 2 mm (one complete turn of the adjusting screw) from the melt and the temperature lowered. The readings were repeated at approximately 30 to 40 degree intervals from approximately 840 down to 720 K. At the end of the run the salt was allowed to cool and a sample was then sent off to analysis to determine the true composition.

Table 1. Comparison of measured values and literature values of conductivities of molten zinc chloride

Temperature (K)	Conductivity (measured) ($\Omega^{-1} m^{-1} \times 10^2$)	Conductivity (Janz [26]) ($\Omega^{-1} m^{-1} \times 10^2$)
822	0.1579	0.1567
798	0.1266	0.1233
772	0.0934	0.0917

3. Results and discussion

3.1. Conductivity

The capillary cells were calibrated at 298 K with 1 D KCl solution and checked over a range of temperature by measuring the conductivity of pure zinc chloride and comparing the values with data from the literature [26]. As can be seen from Table 1, there was good agreement.

The conductivities of twenty-five different compositions in the $ZnCl_2$-KCl-NaCl system were measured at approximately 25 degree intervals from approximately 870 down to 670 K.

The variation in conductivity with temperature was calculated for each of the compositions studied. The results are presented in Table 2 in the form of the constants determined by a linear regression a and b for Equation 7 analysis of the data [3].

$$\kappa = a + bT \tag{7}$$

The variation in conductivity with temperature was then plotted for selected melts (Fig. 2). The general form of these is linear. However, in certain cases, the conductivity decreases more rapidly at low temperatures due to the melt approaching its freezing point and forming large network structures, as described by Bloom and Weeks [3], greatly reducing the number and mobility of the conducting ions and, therefore, causing the conductivity to decrease more rapidly.

$ZnCl_2$-KCl-NaCl ternary diagrams showing contours of equal conductivity were plotted for 773 and
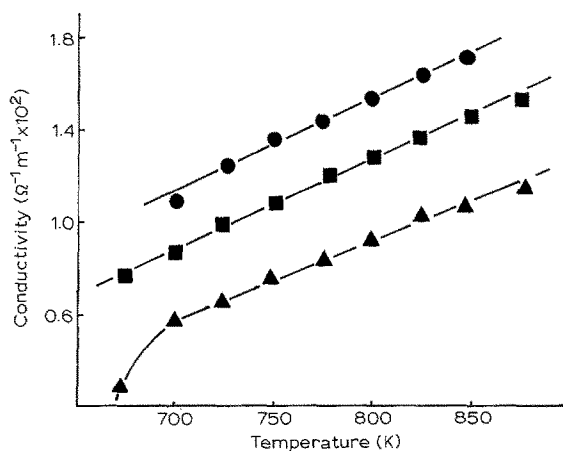
Fig. 2. Variation in conductivity with temperature for selected melt compositions in mol %: (●) 35.7 $ZnCl_2$, 64.3 NaCl; (■) 40.4 $ZnCl_2$, 10.5 KCl, 49.1 NaCl; (△) 28.6 $ZnCl_2$, 54.2 KCl, 17.2 NaCl.

Table 2. The variation in conductivity with temperature for selected $ZnCl_2$-KCl-$NaCl$ melts, expressed as the constants a and b for Equation 7

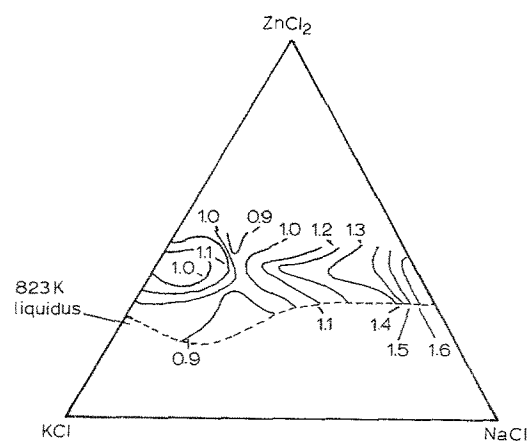| Composition mol%			a $(\Omega^{-1}\,m^{-1} \times 10^2)$	b $(\Omega^{-1}\,m^{-1}\,K^{-1} \times 10^{-1})$	Correlation coefficient
$ZnCl_2$	KCl	NaCl			
50.7	49.3	–	−2.352	4.429	0.000
44.0	45.7	10.3	−1.674	3.290	0.999
46.1	35.1	18.8	−1.472	2.994	0.996
42.9	28.7	28.4	−1.397	2.931	0.997
41.7	13.4	44.9	−1.616	3.512	0.994
44.5	11.9	43.6	−1.753	3.680	0.999
43.1	–	56.9	−2.082	4.474	0.995
42.3	57.7	–	−1.549	3.085	0.997
42.5	45.8	11.7	−1.703	3.369	0.999
41.9	41.2	16.9	−1.232	2.614	0.998
41.5	36.7	21.8	−1.604	3.253	0.999
40.3	30.5	29.2	−1.452	3.218	0.992
40.6	21.4	38.0	−1.811	3.758	0.999
40.4	10.5	49.1	−1.827	3.873	0.998
38.8	–	61.2	−1.963	4.300	0.990
37.9	62.1	–	−1.867	3.526	0.987
40.2	43.2	16.6	−1.684	3.347	0.997
37.4	41.6	21.0	−1.390	2.874	0.999
37.6	29.5	32.9	−1.234	2.870	0.998
36.7	21.9	41.4	−1.424	3.266	0.975
36.1	10.5	53.4	−1.540	3.420	0.999
35.7	–	64.3	−1.636	3.960	0.994
33.4	48.6	18.0	−1.058	2.425	0.990
29.5	60.0	10.5	−1.433	2.919	0.999
28.6	54.2	17.2	−1.784	3.382	0.996

823 K (Figs 3 and 4). The contours were plotted using the data and interpolating, where necessary, assuming local linear variation in conductivity with composition. The overall trend shown in both figures is that of decreasing conductivity as the ratio mol% NaCl increases. A progressively more pronounced ridge occurs in the contours, corresponding to approximately 40 mol% $ZnCl_2$, going from the $ZnCl_2$–NaCl binary to a KCl:NaCl ratio of approximately 3. At this point the ridge meets another which runs around an area of lower conductivity bounded by the $ZnCl_2$–KCl binary.

The expected form of the figures would have been an increase in conductivity as the composition moved to the right and down the diagram, as proportion of mobile Na^+ ions increased and the percentage of less mobile complex ions based on zinc chloride decreased.
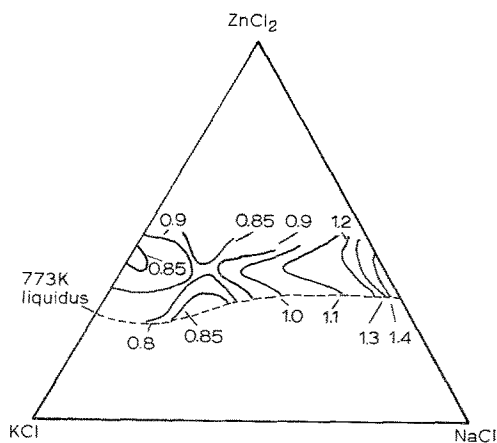
This trend is illustrated to a certain extent in the figures but the origin of the ridges was not initially understood, although the form of the contours for KCl:NaCl ratios of less than 3 is in agreement with work carried out on the variation in cell voltage with composition by Shanks et al. [18]. From the figures, it can be seen that the ridges corresponded closely with the troughs in the liquidus surface (Fig. 5). In these regions the melt has a higher degree of superheat. Therefore, as the conductivity of a melt increases with temperature above its melting point, these compositions have a higher conductivity than might have been predicted without the liquidus curves.

This indicates that the ratio T/T_1, where T is the melt temperature and T_1 is the liquidus temperature, has a significant effect on the conductivity when

Fig. 3. Variation in conductivity ($\Omega^{-1}\,m^{-1} \times 10^{-2}$) with composition at 773 K for the $ZnCl_2$–KCl–NaCl ternary system.
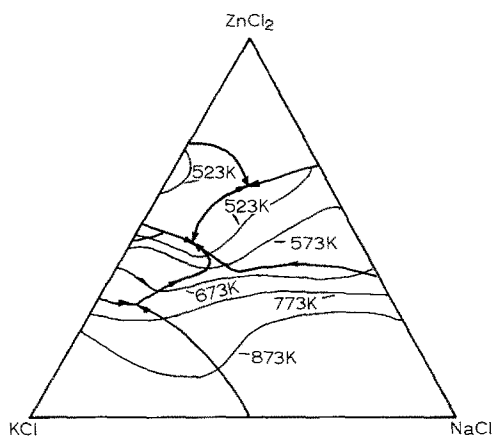

Fig. 4. Variation in conductivity ($\Omega^{-1}\,m^{-1} \times 10^{-2}$) with composition at 823 K for the $ZnCl_2$–KCl–NaCl ternary system.

Fig. 5. Ternary diagram for $ZnCl_2$–KCl–NaCl system [16].

Fig. 7. Variation in density with temperature for selected melt compositions in mol % (●) 49.6 $ZnCl_2$, 33.7 KCl, 16.7 NaCl; (■) 40 $ZnCl_2$, 44.8 KCl, 15.2 NaCl; (▲) 30.4 $ZnCl_2$, 60.0 KCl, 9.6 NaCl.

comparing melts of different composition. This agrees with the literature [2] and explains the significant distortions in the expected trend previously described. It should be noted that T_0 is usually used rather than T_1 when comparing different melts [23, 24, 25]. T_0, which is approximately the glass transition temperature, is the temperature at which the free volume tends to zero. For alkali halides $T_1 = 3 - 3.5T_0$ [24]. In this case it is not possible to correlate the results directly with T_0 as this has not been determined for these melt compositions.

3.2. Surface tension and density

The surface tension and density of ten different compositions in the $ZnCl_2$–KCl–NaCl was measured at 30 to 40 degree intervals from approximately 840 to 720 K. When calculating the density, a correction was made for the displacement of the molten salt by the capillary tubes as a result of the small size of the crucible relative to the outside diameters of tubes [21]. The surface tension and density was calculated at each temperature for each composition using a Commodore CBM model 4032. The standard error in the mean values of the surface tension and the slope of the regression plot for the density were typically 1 and 0.4%, respectively.
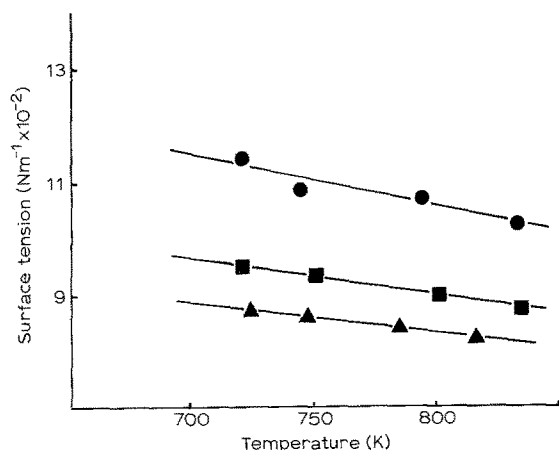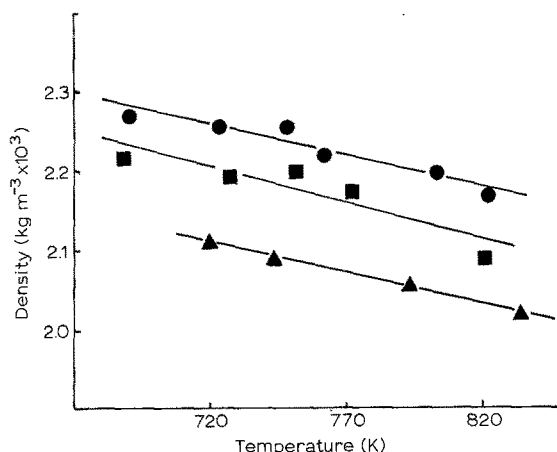
The variation with temperature for both properties was then determined by linear regression analysis, again using the Commodore CBM model 4032, giving the general relationship indicated by Equation 8

$$x = a + bT \tag{8}$$

where $x = \sigma$ or ρ.

The results are presented in the form of the constants a and b , in Tables 3 and 4 for the surface tension and density of each melt composition. The variation in the surface tension and density with temperature was then plotted for selected melts to illustrate the relationship represented by Equation 8 (Figs 6 and 7, respectively).

In order to illustrate the variation with composition, the values of surface tension and density for different melt compositions were plotted on the $ZnCl_2$–KCl–NaCl ternary diagram for 773 and 823 K, together with the data of Cochrane [21].

The variation in surface tension with composition can be seen in Figs 8 and 9. The general trend at both temperatures is of increasing surface tension as the $ZnCl_2$ content decreases down the ternary diagram. There is, however, a step in the contours between approximately 40 and 45% $ZnCl_2$, which develops
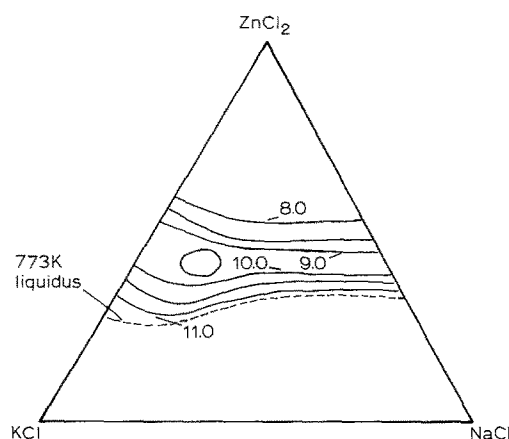

Fig. 6. Variation in surface tension with temperature for selected melt compositions in mol % (●) 30.4 $ZnCl_2$, 60 KCl, 9.6 NaCl; (■) 43.1 $ZnCl_2$, 42.3 KCl, 14.6 NaCl; (▲) 46.5 $ZnCl_2$, 53.5 NaCl.

Fig. 8. Variation in surface tension ($Nm^{-1} \times 10^2$) with composition at 773 K for the $ZnCl_2$–KCl–NaCl ternary system.

Table 3. The variation in surface tension with temperature for selected $ZnCl_2$-KCl-$NaCl$ melts, expressed as the constants a and b for Equation 8

Composition mol %			a (Nm^{-1})	b $(Nm^{-1} K^{-1} \times 10^{-5})$	Correlation coefficient
$ZnCl_2$	KCl	NaCl			
44.6	96.3	9.1	0.342	−31.40	0.976
43.1	42.3	14.6	0.141	−6.27	0.993
40.0	44.8	15.2	0.261	−20.20	0.927
34.2	48.6	17.2	0.149	−6.03	0.999
36.4	36.9	26.7	0.349	−31.60	0.970
30.4	60.0	9.6	0.178	−8.94	0.952
30.0	50.9	19.1	0.142	−4.64	0.988
29.4	48.4	22.2	0.140	−3.93	0.994
46.5	–	53.5	0.126	−5.27	0.984

into a trough in the region of the KCl : NaCl ratio of 1.5.

The general trend of increasing surface tension with decreasing $ZnCl_2$ content agrees with the suggestion that as the melt becomes more ionic the surface tension increases [2]. Initially, the trough was thought to be an artefact due to the limited number of melts examined. However, comparison with the ternary diagram (Fig. 5) shows that the trough coincided approximately with the troughs in the liquidus surface. Melts in these regions have a higher degree of superheat than other melts. The surface tension is therefore lower than might be predicted by considering only the degree of ionic character in the melt, which agrees with the literature [2]. This leads to a temporary levelling off, and local drop in surface tension, which otherwise steadily increases with reducing $ZnCl_2$ content. This point, together with the way in which the surface tension contours generally seem to follow the liquidus contours, again demonstrates the importance of the ratio T/T_1, and hence T_0.

Figures 10 and 11 show the variation in density with composition at 773 and 823 K, respectively. Both figures show a general decrease in density with decrease in $ZnCl_2$ content, with a step in the contours in the region of 35–45% $ZnCl_2$. This general trend agrees with the view that the melt density increases with ion size. Therefore as the proportion of the larger $ZnCl_2$-based ions decreases so the density of the melt

will decrease. The step in the contours was more difficult to explain than in the case of the surface tension. Examination of the contours on the ternary diagram showing the liquidus lines, the step region approximately coincided with the trough in the liquidus surface. However, as the melting point decreases, it would be expected that for a given temperature the density would be less than predicted by simply considering the general trend of decreasing density with decreasing ion size. This would tend to make the density drop more rapidly and bring the contours closer together, rather than spreading them out. The step could be explained by noting that the level region is slightly further down the ternary diagram than in the case of Figs 8 and 9, starting at 35 mol % $ZnCl_2$, rather than 40%. This results in the step coinciding with the area of the liquidus surface in which the melting point is increasing sharply. The ratio T/T_1 is decreasing rapidly in this region and therefore the change in density will tend to be slower than that predicted by the decreasing ion size, resulting in the observed step.

The above explanation could therefore account for the seemingly conflicting trends exhibited by the surface tension and density contours. This point together with the apparent similarity in pattern of the liquidus and density contours confirms the importance of T_1 and hence T_0 when comparing the physicochemical properties of melts with varying composition.

Table 4. The variation in density with temperature for selected $ZnCl_2$-KCl-$NaCl$ melts, expressed as the constants a and b for Equation 8

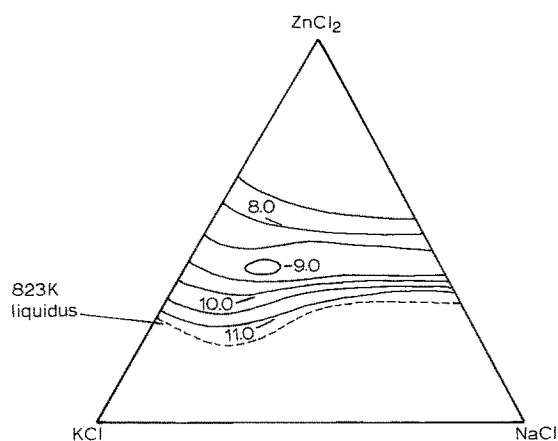| Composition mol %			a $(kg\,m^{-3} \times 10^3)$	b $(kg\,m^{-3} K^{-1})$	Correlation coefficient
$ZnCl_2$	KCl	NaCl			
44.6	96.3	9.1	3.38	−1.501	0.974
43.1	42.3	14.6	2.79	−0.787	0.989
40.0	44.8	15.2	2.85	−0.815	0.961
34.2	48.6	17.2	2.89	−0.951	0.912
36.4	36.9	26.7	2.73	−0.749	0.998
30.4	60.0	9.6	2.94	−1.022	0.924
30.0	50.9	19.1	2.70	−0.823	0.989
29.4	48.4	22.2	2.93	−1.163	0.999
46.5	–	53.5	2.57	−0.682	0.876
			2.94	−0.876	0.941

Fig. 9. Variation in surface tension ($Nm^{-1} \times 10^{-2}$) with composition at 823 K for the $ZnCl_2$-KCl-NaCl ternary system.
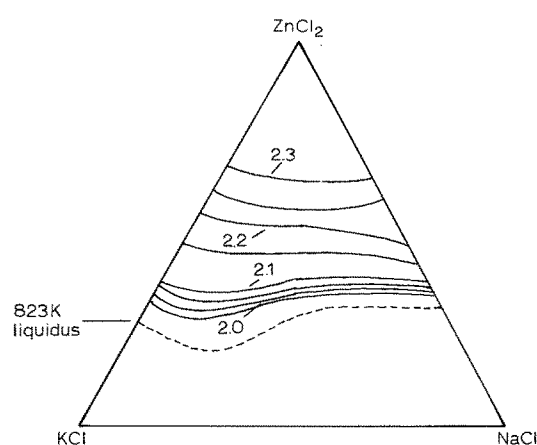
Fig. 11. Variation in density ($kg\,m^{-1} \times 10^3$) with composition at 823 K for the $ZnCl_2$-KCl-NaCl ternary system.

4. Conclusions

The variation in conductivity, surface tension and density with the temperature and composition of the $ZnCl_2$-KCl-NaCl melts agreed in general with the behaviour predicted by the literature. The most significant point to note was the apparent importance of T_1, and hence T_0, on the shape of the contours of all three properties when plotting their variation with melt compositions on the $ZnCl_2$-KCl-NaCl ternary diagram.

When considering the optimum melt to use in an electrolysis cell, the conductivity should be as high as possible. The best composition would therefore be the binary 35% $ZnCl_2$, 65% NaCl (in mol %).

The surface tension of interfacial tension between the gas and the melt should be as high as possible to reduce the chance of forming small gas bubbles which would mix more readily and lead to increased recombination. Therefore, the most suitable composition would be approximately 27% $ZnCl_2$, 61% KCl, 12% NaCl (in mol %). Note that the gas used in these experiments was inert argon rather than the chlorine which is produced during electrolysis.

The density difference between the electrolyte and the metal should be large enough to allow good separation. In this case the difference in density between the melt and the metal is approximately $5000\,kg\,m^{-3}$, which is considerably larger than the variation in density with composition, which is of the order of $250\,kg\,m^{-3}$. Therefore, from the point of view of density differences, the melt composition is of little significance.

The melt should have a reasonable superheat to avoid freezing. Excessive fuming should also be avoided. Therefore reasonable margins should be allowed for variations in both temperature and composition during electrolysis. Based on the literature, the temperature should be approximately 770 K and the KCl : NaCl ratio should be greater than or equal to one. Considering all of the above factors, the optimum melt should have a composition of approximately: 40 mol % $ZnCl_2$, 30 mol % KCl, and 30 mol % NaCl.

5. Acknowledgements

Fig. 10. Variation in density ($kg\,m^{-3} \times 10^3$) with composition at 773 K for the $ZnCl_2$-KCl-NaCl ternary system.

References

[1] IU. K. Delimarskii and B. F. Markov, 'Elecrochemistry of Fused Salts', Sigma Press (1961).
[2] H. Bloom, 'The Chemistry of Molten Salts', W. A. Benjamin Inc., New York (1967).
[3] H. Bloom and I. A. Weeks, Trans. Faraday Soc. 61 (1971), 1416.
[4] C. B. Alcock, 'Principles of Pyrometallurgy', Academic Press, New York (1976).
[5] E. R. van Artsdalen and I. S. Yaffe, J. Phys. Chem. 59 (1955) 118.
[6] F. R. Duke and A. R. Fleming, J. Electrochem. Soc. 104 (1957) 251.
[7] D. G. Lovering, 'Molten Salt Technology', Plenum Press, New York (1982).
[8] G. Mamantov (ed.), 'Molten Salts', Marcel Dekker, New York (1969).
[9] B. R. Sundheim (ed.) 'Fused Salts', McGraw-Hill, London (1964).
[10] J. L. Dahl and F. R. Duke, J. Phys. Chem. 62 (1958) 1142.
[11] Idem, ibid. 62 (1958) 1498.
[12] G. Bertizei and G. Stenheim, ibid. 68 (1964) 2909.
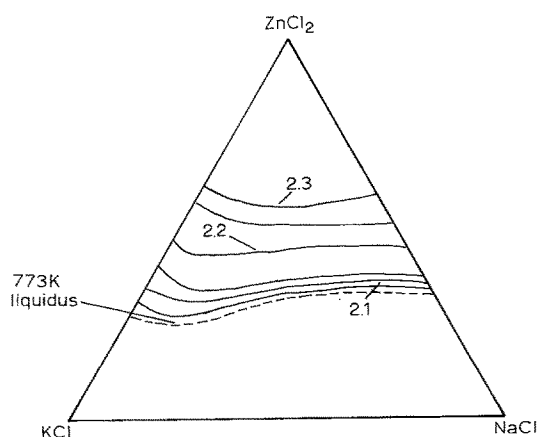[13] H. Reiss and S. W. Mayer, ibid. 34 (1961) 2001.

[14] E. N. Hodkin and M. G. Nicholas, *J. Nucl. Mater.* **43** (1972) 308.

[15] K. Grjotheim *et al.*, 'Aluminium Electrolysis', Spottiswoode Ballantyre Press, London (1977).

[16] M. M. Wong and F. P. Haver, 'Molten Salt Electrolysis in Metal Production', IMM (1977).

[17] F. P. Haver, D. E. Shanks, D. L. Bivey and M. M. Wong, US Bureau of Mines, R.I. 8133 (1976).

[18] D. E. Shanks, F. P. Haver, C. H. Elges and M. M. Wong, US Bureau of Mines, R.I. 8343 (1979).

[19] J. O'M. Bockris, J. L. White and J. D. Mackenzie, "Physicochemical Measurements at High Temperatures', Butterworths Scientific Publications, London (1959).

[20] H. J. Gardner, C. T. Brown and G. J. Janz, *J. Phys. Chem.* **60** (1956) 1458.

[21] R. F. Cochrane, Ph.D. thesis, Cambridge University (1986).

[22] R. C. Weart (ed.), 'Handbook of Chemistry and Physics', CRC Press, Cleveland (1977).

[23] C. A. Angell, *J. Phys. Chem.* **68** (1964) 1917.

[24] *Idem, ibid.* **69** (1965) 399.

[25] H. Bloom and I. A. Weeks, *Trans. Faraday Soc.* **67** (1971) 1410.

[26] G. J. Janz, 'Molten Salts Handbook', Academic Press, New York (1967).